JOURNAL OF OPTOELECTRONICS AND ADVANCED MATERIALS Vol. 9, No. 4, April 2007, p. 902 - 906

Droplet dispersion calculations for ultrasonic spray pyrolysis depositions

D. CHAPRON*, M. GIRTAN[a], J.-Y. LE POMMELEC, A. BOUTEVILLE
LPMI, ENSAM, Angers, France
[a]*POMA, Université d'Angers, France*

Spray-CVD is a low cost deposition technique with high efficiency at atmospheric pressure. The thin films quality depends on the deposition parameters: the temperature profile of the substrate, the carrier gas flow rate, the nature of the starting solution, the droplets diameter dispersion, etc… In previous numerical simulation, the optimized carrier gas flow [1] and the temperature profile [2] of our horizontal spray pyrolysis setup have been carried out. The aim of this contribution is to study the correlation of these parameters with injected droplets of the starting solution. The selectivity of the reactor geometry with respect to the droplets diameter dispersion is presented. Then, the optimized deposition parameters calculated by Computational Fluid Dynamics (CFD) simulation for this configuration are demonstrated.

(Received November 2, 2006; accepted February 28, 2007)

Keywords: Droplet dispersion, Numerical simulation, Spray-CVD

1. Introduction

In order to improve the thin films quality, numerical simulations are essential to understand all physical processes which take place in the reactor of a deposition system. In most of the deposition techniques, as for Spray-CVD, the temperature profile homogeneity of the substrate is the critical point.

Spray pyrolysis has cost effectiveness, large area application and easy doping. This technique involves spraying of a solution containing precursor salts onto a substrate at an elevated temperature. The spraying droplets reaching the hot substrate surface undergo pyrolytic decomposition and form a crystalline film. The physical intrinsic parameters of the mist, droplets velocities and diameters, are difficult to measure during the deposition and also need to be optimized. Consequently, the aim of our investigation was to simulate the droplets behaviour in our horizontal spray reactor for different carrier gas flow rates.

2. Experimental setup

The 2D geometry of the experimental apparatus is shown in Fig. 1. It is mainly consisted of two parts. The first one is the injection part. Droplets are generated by an ultrasonic oscillator which is placed in a solution. Here, the used solvent containing the precursors is ethanol. Air is used as the carrier gas to accompany the atomized droplets into the deposition part. This second zone is surrounded by a quartz tube, within an inclined silicon susceptor is heated by three infrared lamps. The thickness of the quartz substrate, placed on the susceptor, is 1mm. The solvent evaporates above and onto the substrate and the dissolved substances react to form the reactional product.

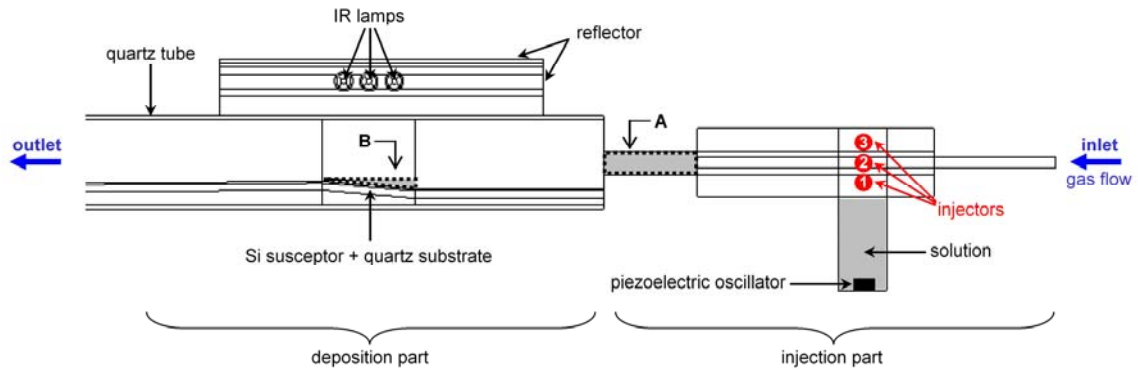

Fig. 1. Spray-CVD setup.

In previous numerical simulations, the velocity profile of the carrier gas flow close to the substrate [1] and the temperature profile of the substrate [2] have been determined. It has been shown that a substrate inclination

of 5° and a flow rate of 2L.min^{-1} was the optimized geometrical arrangement.

These calculations did not take account of the spray. Consequently, we have investigated the behaviour of injected droplets for this substrate inclination with different gas flow rate in such a geometry.

3. Spray computational modelling

Simulations are performed using the finite volume commercial computational fluid dynamics software CFD-ACE [3].

The motion equation of a droplet surrounded by a fluid in a gravitational field is:

$$m_d \frac{\partial v}{\partial t} = C_D \rho_f [U - v] |U - v| \frac{A_d}{2} + m_d g \qquad (1)$$

m_d is the mass of the droplet, v its velocity vector, A_d its frontal area and C_D its drag coefficient. ρ_f and U are the density and the velocity vector of the fluid respectively. This equation is coupled with the surrounding fluid parameters driving by standard Navier-Stockes equations.

These differential equations, describing the mass conservation of the carrier gas flow and of the accompanying liquid with the total energy conservation of the system, are solved. For dynamic calculations, other forces exerted upon droplets have been taken into account: Saffman lift force, pressure gradient force and Brownian motion force. Indeed, piezoelectric oscillators generate micronic droplets resulting in non negligible Brownian force, F_B, which considers collisions between gas molecules and small droplets [4]:

$$F_B = R \sqrt{\frac{216}{\pi} \frac{\mu_f k_B T}{C_C \rho_f{}^2 d_d^2 \Delta t}} \qquad (2)$$

Cc is the Cunningham correction factor, μ_f is the dynamic viscosity. T is the absolute temperature, Δt is the time step and R is the Gaussian random number bounded by -1 and +1.

Small liquid droplets can be generated by different injection systems. Two of them are mostly used: pneumatic, through a nozzle and ultrasonic with a piezoelectric oscillator. The diameter dispersion of the droplets obeys to the Rosin-Rammler law for the generation from a nozzle [5] and to a log-normal law for the ultrasonic one [6].

For ultrasonic atomization, the diameter of the generated droplets d_d can be expressed as [7]:

$$d_d = 0{,}34 . \left[\frac{8\pi\sigma_{liq}}{\rho_{liq} f^2} \right]^{1/3} \qquad (3)$$

f is the frequency of the ultrasonic vibration, σ_{liq} and ρ_{liq} are the surface tension and the density of the liquid respectively.

Ultrasonic waves involve the appearance of a stream above the solution. The droplets are generated from this fountain jet in all the injector height. To simplify the simulation of this stream, three identical point injectors are used (Fig. 1). First, the injector 2 is placed in the center of the injected gas flow. Then, the injectors 1 and 3 are localized under and above the inlet injection respectively.

To highlight the evolution of the droplets distribution during their transport onto the substrate, the injected ethanol droplets have an identical discrete square distribution of their diameters between 1µm and 16µm for all the point injectors (Fig. 2). Also to reduce the calculation time, droplets in contact with walls are destroyed and no thermal interaction is considered between droplets and their surrounding medium.

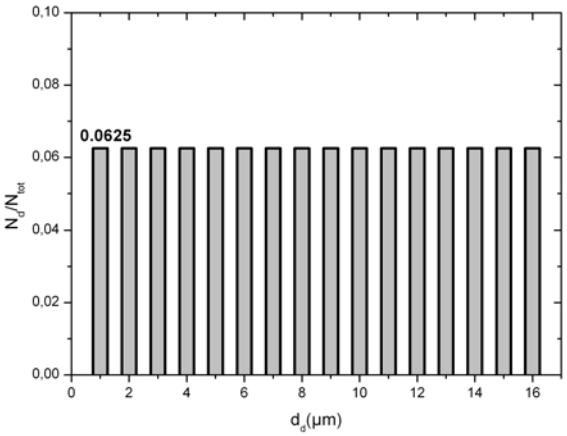

Fig. 2 – Discrete diameter distribution of the injected droplets by the point injectors 1, 2 and 3. N_d is the number of generated droplets with the diameter d_d. N_{tot} is the total number of injected droplets.

4. Results and discussion

We first report in Fig. 3 the calculations results in steady state of the velocity vector magnitude of the carrier gas flow, U, for an air flow rate inlet of 5L.min^{-1}. The average velocity near the substrate surface is found around 2×10^{-3}m.s^{-1}. The droplets trajectories calculations from this initial flow state are presented in Fig. 4. Parcels are injected at a rate of 10 per second for the three injectors. The number of droplets per parcel is dependent on the droplet diameter to respect the accompanying liquid mass conservation.

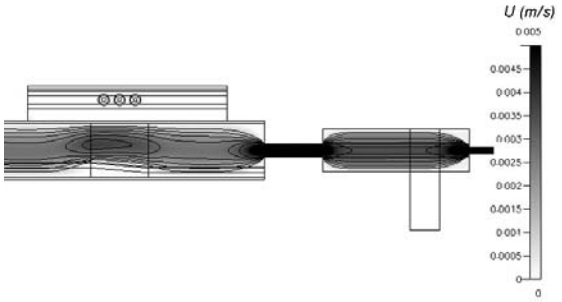

Fig. 3. Gas velocity magnitude of the carrier gas for an air flow rate U of 5 L.min^{-1}.

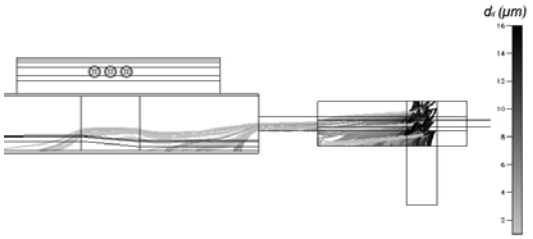

Fig. 4. Droplets trajectories versus their diameters d_d. The inlet gas flow rate U is 5 L.min^{-1}.

The droplets trajectories depend strongly on their diameters. Large droplets, represented in dark grey, stay in the injector part of the apparatus. Droplets with a diameter around 5µm stayed in the first part of the quartz tube. Only light droplets, with a diameter below 4µm, come onto the substrate.

Moreover, most of the droplets which enter in the deposition part are injected by the top point injector (injector 3). All droplets injected by the point injector 1, can not get over the injector output. They are supposed to return into the start solution after a collision with walls. Only the small droplets of the point injector 2, localized in the flow center, pass thought the output and go in the deposition part.

Then, in this horizontal setup a selection of the small droplets is done. It is clear that in a vertical spray configuration the diameter distribution of the droplets, which come onto the substrate, is identical to the droplets distribution of injectors. Also with these results, considering the ultrasonic atomization selectivity, we can affirm that our horizontal injection configuration induced close selection of the droplets which come on the substrate.

In order to distinguished calculation results, two particular areas are studied (Fig. 1). The first area is at the output of the injector, it is presented as the area A. The effective droplets which pass through this zone enter in the deposition part. The second area, area B, is a small zone located above the substrate. All the droplets which are in this zone are considered to be effective for the chemical reaction onto the substrate.

The temporal evolutions of the droplets flow rates in these two zones are represented in Fig. 5. The initial time is the starting droplets injection by the three point injectors. The carrier gas flow, in steady state, is taken as initials conditions. After 25s, first droplets arrived in the injector outlet (zone A). Then, the flow rate Q_w^A increases rapidly until 40s. The steady state is then reached.

The variation of the droplets flow rate onto the substrate is plotted in Fig. 5. The slow increase of Q_w^B from 75s is due to the first light droplets which arrived into the substrate. Their contribution to Q_w^B is low. The steady state of the system in area B is reached after two minutes.

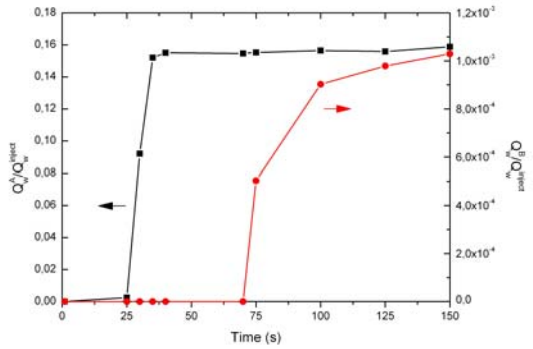

Fig. 5. Temporal evolution of the droplets flow rates in the injector, Q_w^A, and close to the substrate, Q_w^B, for Q_v = 5L.min^{-1}. The results are normalized with the total injected droplets flow rate Q_w^{inject}.

The droplets diameter dispersion for the air flow rates 1L.min^{-1}, 3L.min^{-1} and 10L.min^{-1} in steady state at the injector output are plotted in *Fig. 6*. For all carrier gas flow rates, the initial square distribution is lost. It shows that only small droplets can enter in the deposition part. Droplets with diameters beyond 5µm are filtered. Similar distributions of the droplets are shown with the increase of the air flow rate. Therefore, the first selection of the effective droplets is done by the injector geometry.

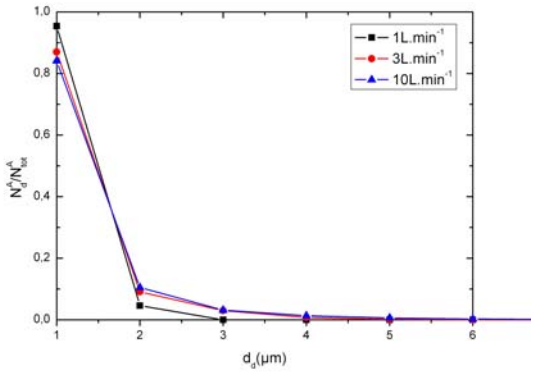

Fig. 6. Diameter dispersion of the droplets for the gas flow rates 1, 3 and 10L.min^{-1} at the injector output (zone A). N_d^A/N_{tot}^A represents the ratio of the droplets number at the diameter d_d versus the all present droplets in the area A.

The integration of the droplets mass, M_d^A, and the integration of the ratio of their flow rate, Q_w^A, on the injected droplets flow rate in the injector output (area A), Q_w^{inject}, versus the carrier gas flow, Q_v, are presented in Fig. 7. The value of M_d^A has been shown to be linearly dependant upon Q_v. The variation of M_d with the carrier gas flow is divided in two parts. In the first one, for Q_v below 5L.min^{-1}, the total mass of the droplets which are in the injector output decreases when the carrier air flow increases. Indeed, at low gas velocities, only the droplets from the point injector 3 are in the area A. Droplets which are generated in the bottom part and in the flow center of the injector are filtered. Then, when Q_v increases the density of the droplets in the area A decreases because of the droplets injected flow rate conservation.

For a gas flow rate superior to 5L.min^{-1}, a large part of the injected droplets are transported by the carrier gas and the small ones injected by the injector 2 get over the injector output. Then the total droplets mass increases with the carrier gas velocity.

The evolution of the ratio Q_w^A/Q_w^{inject} is represented in Fig. 7. As the gas velocity increases, the rate of the accompanying liquid becomes higher. Two linear phases can be distinguished. As we have seen, below 5L.min^{-1}, only the droplets generated by the point injector 3 participate to the accompanying liquid flow rate. The linear fit gives a slope of 0.04 min.L^{-1}. Beyond 5L.min^{-1}, the injector 2 has a contribution in the droplets flow rate. A double slope, resulting from the linear fit, emphases this contribution. At 10L.min^{-1}, most of the droplets injected by the injectors 2 and 3 go in the injector outlet and can participate to the deposition process.

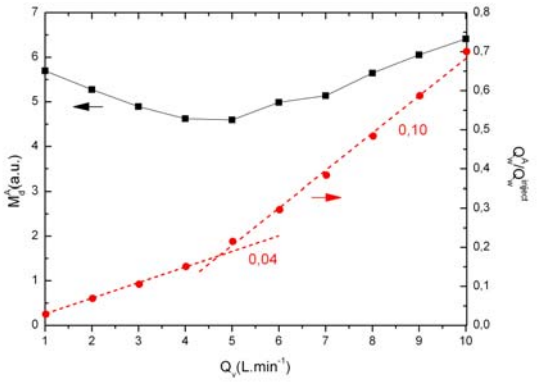

Fig. 7. Variations of the droplets total mass M_d^A and their flow rate Q_w^A/Q_w^{inject} (area A), normalized on the injected droplets flow rate in the injector, versus the carrier gas flow Q_v.

After the analyse of the droplets diameter distribution in the injector output, which are effective to participate to the deposition process, the same study in the area B close to the substrate has been done.

The droplets diameter dispersion for the air flow rates 1L.min^{-1}, 3L.min^{-1} and 10L.min^{-1} are reported in *Fig. 8*. At 1L.min^{-1}, no droplet is present onto the substrate. As the gas flow rate increases the proportion of small droplets onto the substrate increases. The droplets start to arrive on the substrate for a gas flow rate threshold of 3L.min^{-1}. At this flow rate, only 1 µm droplets are in the area B. For higher carrier gas flow rates larger diameter dispersion is observed. However, the major part of droplets onto the substrate consists of thin ones with a diameter of 3µm and lower.

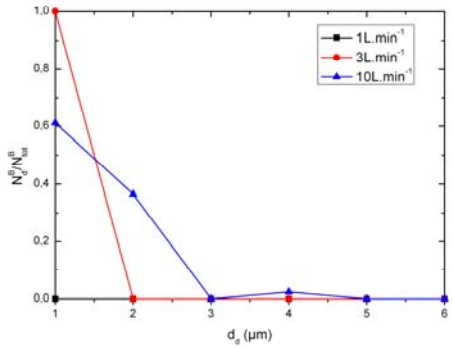

Fig. 8. Diameter dispersion of the droplets for the gas flow rates 1, 3 and 10L.min^{-1} onto the substrate (zone B). N_d^B/N_{tot}^B represents the ratio of the droplets number at the diameter d_d versus the all present droplets in the area B.

The variation of the total droplets mass M_d^B in area B is provided in Fig. 9. First, the irregular evolution of M_d^B is due to the discrete distribution of initial injected droplets. Until 4L.min^{-1}, the mass of droplets increases with the increase of the carrier gas flow rate. Then, M_d^B decreases, because a part of the 1µm droplets are carried over the substrate. The higher density of the arrivals droplets and the contributions of large droplets from injectors 2 and 3 entail the increase of M_d^B from 7L.min^{-1}.

The similar behaviours of M_d^B *and* Q_w^B indicate that in the deposition part, the geometry doesn't participate to the droplets diameter segregation.

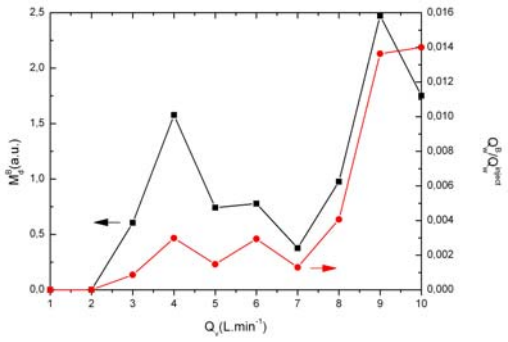

Fig. 9. Variations of the droplets total mass M_d^B and their flow rate Q_w^B/Q_w^{inject} (area B), normalized on the injected droplets flow rate above the substrate, versus the carrier gas flow Q_v.

The optimized configuration for a close droplets diameter dispersion above the substrate is to have a low carrier gas flow. Around 3L.min^{-1} is ideal and compatible with the flow rate of 2L.min^{-1} found in our previous calculations to obtain a uniform velocity profile [1].

5. Conclusions

The old spray pyrolysis technique principle is always a topical deposition process because of all its advantages. The present study shows the calculations of the sprayed droplets trajectories in a horizontal setup for various carrier gas flow rates.

These results reveal that the spray propagation implies a strong size selection of the effective droplets. Only small droplets, with micronic diameters, can reach the substrate. Or, good deposition conditions need small droplets. Indeed, when the droplets are thin, the thermal shocks between them and the hot substrate are limited. Or, the temperature of the substrate needs to be homogeneous and constant during all the deposition process. Moreover, with a close diameter dispersion the amount of reactive compounds reaching the substrate is regular and homogeneous, which could improve the quality of deposited films.

The other interesting point of this study is that the stream of precursors must take all the injector area. At low carrier gas flow, only generated droplets from the top of the injector, above the carrier gas flow inlet, reach the substrate.

This work will be useful to optimize spray pyrolysis systems from the point of view of the mist parameters. As further work, the effect of the temperature profile of the reactor on the droplets trajectories will be performed.

References

[1] M. Girtan, P. O. Logerais, A. Bouteville, Proceeding, EUROCVD - 15, September 4-9 (2005), Bochum – Germany.
[2] M. Girtan, P. O. Logerais, A. Bouteville, J. Optoelectron. Adv. Mater. **8**(1), 144 (2006).
[3] CFD'ACE software is an ESI group product, Huntsville, USA (www.esi-group.com).
[4] A. Li, G. Ahmadi, Aerosol Sci. Technol., **16**(4), 209 (1992).
[5] S. S Yoon, J. C. Hewson, P. E. DesJardin, D. J. Glaze, A.R. Black, R. R. Skaggs, Int. J. of Multiphase Flow, **30**, 1369 (2004).
[6] Y. Bando, S. Yamaguchi, K. Doi, M. Nakamura, K. Yasuda, A. Oda, and Y. Kawase, J. of Chem. Eng. of Japan, **37**(10), 1286 (2004).
[7] R. T. Lang, J. Acoust. Soc. Am. **34**(6) (1962).

*Corresponding author: David.Chapron@angers.ensam.fr